Adsorption of L-DOPA Intercalated in Hydrated Na-Saponite Clay: A Combined Experimental and Theoretical Study

ARTICLE *in* THE JOURNAL OF PHYSICAL CHEMISTRY C · DECEMBER 2012

Impact Factor: 4.77 · DOI: 10.1021/jp3094148

7 AUTHORS, INCLUDING:

Vicente Timón
Spanish National Research Council
31 PUBLICATIONS **280** CITATIONS
SEE PROFILE

Jean-François Lambert
Pierre and Marie Curie University - Paris 6
151 PUBLICATIONS **2,663** CITATIONS
SEE PROFILE

Maguy Jaber
Pierre and Marie Curie University - Paris 6
85 PUBLICATIONS **555** CITATIONS
SEE PROFILE

Frederik Tielens
Collège de France
93 PUBLICATIONS **1,330** CITATIONS
SEE PROFILE

THE JOURNAL OF PHYSICAL CHEMISTRY C

Article

pubs.acs.org/JPCC

Adsorption of L-DOPA Intercalated in Hydrated Na-Saponite Clay: A Combined Experimental and Theoretical Study

Khaled El Adraa,[†,‡] Vicente Timon,*[,†,‡,§] Jean-François Lambert,[†,‡] Abdel-Rahman Al-Rabaa,[∥] Farouk Jaber,[∥,⊥] Maguy Jaber,[†,‡] and Frederik Tielens*[,†,‡]

[†]UPMC Univ Paris 06, UMR 7197 and [‡]CNRS, UMR 7197, Laboratoire de Réactivité de Surface, Casier 178, 4, Place Jussieu, F-75005 Paris, France

[§]CSIC, Instituto Andaluz de Ciencias de la Tierra, Fuentenueva 1, 18001 Granada, Spain

[∥]Laboratoire d'Analyse des Composés Organiques (509), Univ. Libanaise − Campus Universitaire de Rafic HARIRI, Faculté des Sciences I. Dép. de Chimie et de Biochimie, Beyrouth, Liban

[⊥]Laboratoire d'Analyse de Pesticides et de Polluants Organiques, Commission Libanaise de l'Energie Atomique, B. P. 11- 8281, Riad El Solh, 1107 2260 Beyrouth − Liban

ABSTRACT: The intercalation of L-DOPA into the interlayer space of saponite, a 2:1 phyllosilicate, and the nature of host−guest interactions are investigated by a combined experimental and theoretical approach. L-DOPA zwitterions are accommodated vertically in the interlayer region as a bilayer of partially interdigitated species. The hydration state of the nanocomposite as well as the interaction geometry of L-DOPA molecules in the clay interlayer, are determined by periodic DFT calculations and found to be in agreement with experimentally obtained data. New insights into the transport properties for biomolecules in saponite are discussed.

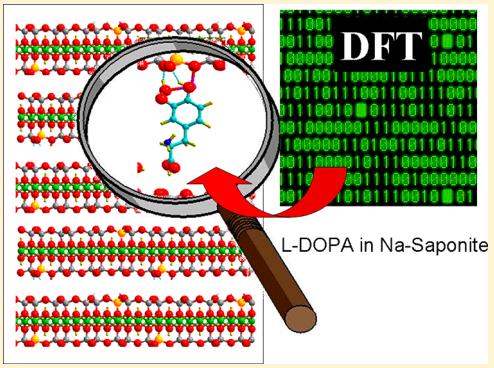

1. INTRODUCTION

An important property of smectite clay minerals is their ability to adsorb water in large amounts in their interlayer space, thereby resulting in a size expansion of several times their initial thickness. This process is known as clay swelling and plays a key role in various processes such as in mud-rock drilling for oil and gas production.[1,2]

Swelling is only one example of topotactic intercalation reactions. In the world of hybrid materials, clays and clay minerals occupy a special place because they are readily available at low cost while constituting a very specific type of matrix for the structuring of organic components. Namely, they are made of extended 2D layers that can rather easily be separated from each other and therefore provide a 2D constrained space with tunable thickness. The intercalation of organic molecules in this constrained space, the interlayer, easily provides a specific type of nanocomposites, in which inorganic and organic components regularly alternate on the nanometric scale.[3]

One group of bio-organic molecules, the amino acids and their derivates, play a major role in life as building blocks of biopolymers such as proteins and are used in many industrial applications, especially in adsorption, separation, and vectorization of organic molecules.[4,5] Over the years, many studies have investigated the intercalation of amino acids or other related molecules into clays for various purposes (see, e.g., refs 6−15).

In particular, the adsorption and reactivity of amino acids into clay minerals have been widely studied because clays may have played an important role in chemical evolution and the origin of life on earth (refs 16 and 17 and references cited therein).

Amino acids are also of central importance in pharmacology. Among them, L-DOPA (L-3,4-dihydroxyphenylalanine), as the precursor of dopamine, is an important neurotransmitter that is commonly used for the treatment of neural disorders such as Parkinson's syndrome.[18−20] After oral administration, L-DOPA is rapidly absorbed through the bowel, then converted to dopamine by DOPA−decarboxylase.[21,22] Side effects appear if L-DOPA is taken at high dosages.[23] To avoid these and for better regulation of DOPA uptake, it would be interesting to vectorize it on inorganic matrices that might result in delayed or controlled release. Indeed, vectorization of L-DOPA or of the related dopamine has been attempted by several authors; most relevant to the present work, the intercalation of L-DOPA has been studied in a layered material, Mg/Al-LDH.[24] Recently our group investigated L-DOPA interaction with two different trioctahedral smectites, saponite and laponite, as well as an amorphous silica (Aerosil 380).[25,26] This was found to be

Received: September 21, 2012
Revised: November 19, 2012

   dx.doi.org/10.1021/jp3094148 | J. Phys. Chem. C XXXX, XXX, XXX−XXX

complicated by the co-occurrence of oxidative polymerization reactions to a material resembling melanin, as reported by others.[27]

Here we present results on the adsorption of L-DOPA into Na-saponite under hydrated and dehydrated conditions. This work is in line with former studies on the characterization of bio-organic molecules on silica-based materials.[28−30]

Theoretical methods based on the density functional theory and molecular dynamics are employed nowadays to understand and predict several of the above-mentioned phenomena. The importance of theoretical chemistry for intercalated materials is critical because little structural and physical data is available due the nanoscale heterogeneity of these hybrids and the lack of good quality single crystals for diffraction-based characterization and analysis. In this study, the interaction between expandable clay and a bio-organic molecule derived from an amino acid is investigated, with the aim to understand the early stage interactions among amino acid groups inside a hydrated clay interlayer.

Previous theoretical studies involving clays and amino acids are rather rare. They have investigated the structure and arrangement of chiral amino acids D-histidine or L-histidine in a hydrated clay,[31] the catalytic stereoselectivity in adsorption and subsequent reactions of dipeptide stereoisomers forming amide bonds in montmorillonite,[32] and the prebiotic selection and organization of biomolecules.[33] Some theoretical studies that do not directly involve amino acids, but rather nucleobases, are also relevant because similar adsorption mechanisms may be at play.[33]

2. EXPERIMENTAL PART

Na-saponite was synthesized according to a previously published procedure,[34] having the following chemical formula:

$$Na_{0.8}[Si_{7,2}Al_{0.8})(Mg_6)O_{20}(OH, F)_4] \quad (1)$$

That is, the Al substitution rate expressed per full unit cell is x = 0.8.

L-DOPA (3,4-dihydroxy-L-phenylalanine, 99.99 wt %) was purchased from Sigma Aldrich. A 2% (w/w) saponite dispersion was prepared in a 2.70 × 10^{-2} mol L^{-1} aqueous solution of L-DOPA, and the resulting dispersion was stirred for 24 h at room temperature. The pH of the medium was 7.5. The solid was then separated by filtration and dried for 48 h at 60 °C.

X-ray powder diffraction (XRD) was carried out on the final solids with a Bruker D8 Avance diffractometer using the Cu Ka radiation (wavelength λ = 1.5404 Å). The XRD patterns were recorded between 3 and 70° with a step size of 0.05° and have been discussed elsewhere[25] together with TEM characterization. Thermogravimetric analysis (TGA) of the samples was carried out on a TA Instruments − Waters SDT Q600 analyzer with a heating rate of 5 °C min^{-1} under dry air flow (100 mL min^{-1}). Prior to thermal analysis, samples were dehydrated by oven-drying (303 K) and then rehydrated under controlled humidity (80%).

3. THEORY AND COMPUTATIONAL DETAILS

a. Model. The Na-saponite model is constructed started from the crystal structure of saponite. Saponite clay minerals have a general formula $Na_x(Si_{8-x}Al_x)(Mg_6)O_{20}(OH)_4$, where x = 0.2 to 1.2. The synthetic saponite used in the experimental part has x = 0.8 (see eq 1), but the degree of substitution in the model cannot be varied continuously due to the finite size of the unit cell. Therefore, the formula of bulk Na-saponite unit cell used is the proposed model is the following:

$$NaSi_7AlMg_6O_{20}(OH)_4 \quad (2)$$

In other words, x is set equal to 1, slightly overestimating the Al and Na content, which gives a unit cell with a reasonable number of atoms and geometric size.

The model consists in a (1 × 2 × 1) supercell (see Figure 1), with the following general formula:

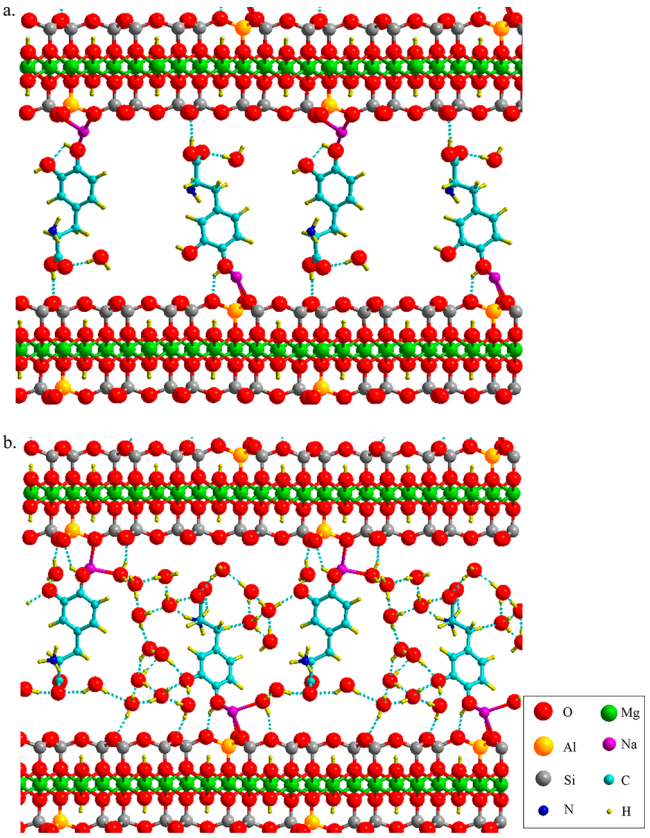

Figure 1. Optimized saponite (1 × 2 × 1) cell showing possible hydrogen-bond interactions (dashed black lines) in a models (a) containing L-DOPA and 1 water molecule and (b) and L-DOPA and 10 water molecules.

$$Na_2Si_{14}Al_2Mg_{12}O_{40}(OH)_8 \quad (3)$$

Once the clay model is built, the interlayer space is expanded to introduce the water molecules and L-DOPA, as observed experimentally:[25,26,35,36] swelling attributable to DOPA intercalation has been evidenced by XRD as reported in a previous presentation.[25]

To study the effect of hydration, we added 2 to 20 water molecules in the double unit cell, and the structures were then optimized, which results in adding a maximum of 10 water molecules per unit cell.

Different geometries are possible for the introduction of L-DOPA inside the clay. Two L-DOPA molecules are added in the model (double unit cell, that is, one DOPA molecule per unit cell), one pointing up and another pointing down in the interlayer space to preserve the symmetry. (See Figure 2.)

In summary, the DOPA−saponite model is constituted of eight different atomic species, H, C, N, O, Na, Mg, Al, and Si,

dx.doi.org/10.1021/jp3094148 | J. Phys. Chem. C XXXX, XXX, XXX−XXX

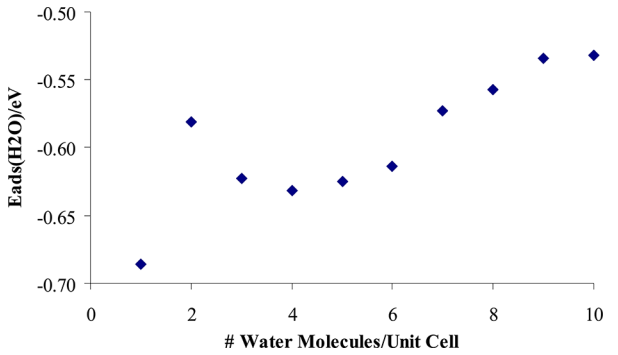

Figure 2. Calculated adsorption energy of a single water molecule within the clay layers versus the number of water molecules present in the unit cell.

and contains from 136 to 196 atoms, depending on the number of water molecules considered.

One should notice that theoretical results concern only the intercalated layers. The relative proportion of intercalated versus unintercalated layers cannot be addressed due to the small scale of the supercell.

b. Computational Details. The geometry optimization and minimization of the total energy are performed using the VASP code.[37,38] In the periodic density functional theory framework used, the Kohn–Sham equations are solved by means of the PW91[39] and PBE functionals,[40,41] already used in former studies.[42−46] The electron–ion interaction is described by the projector augmented-wave method (PAW).[47,48]

All atom positions and cell parameters of the model are relaxed without geometrical constraints. Optimizations are performed using a Monkhorst-Pack k-point mesh of 6 × 2 × 1, giving a total of 8 k-points for the Brillouin-zone integration. The energy cutoff is of 500 eV, and the potential energy is determined by the full quantum mechanical electronic structure until the total energy differences between the loops is $<10^{-4}$ eV.

One drawback of classical DFT methods is that dispersion interactions are not taken into account. In our systems, it is expected that pure electrostatic forces will dominate compared with the dispersion forces due to the presence of water molecules.

The adsorption energy ΔE_{ads} of water is calculated using eq 4:

$$\Delta E_{ads} = E_{syst} - (E_{sapo} + nE_{H_2O}) \quad (4)$$

where E_{syst}, E_{sapo}, and E_{H_2O} represent the total energy of the system containing n water molecules, the total energy of the system without water, and the total energy of the water molecules, respectively.

Also, the adsorption energy per L-DOPA molecule in the saponite clay is calculated using eq 5:

$$\Delta E_{ads} = \frac{1}{2}(E_{syst} - (E_{sapo.hydr.} + 2E_{DOPA})) \quad (5)$$

where E_{syst}, $E_{sapo\_hydr.}$, and E_{DOPA} represent the total energy of the system containing n water molecules and two DOPA molecules, the total energy of the system with n water molecules, and the total energy of the L-DOPA molecule, respectively.

4. RESULTS AND DISCUSSION

Experimental Data. XRD patterns revealed[25] the expected (hkl) saponite reflections. In the raw saponite, the (001) reflection is observed at 6.2° (2θ) and corresponds to a $d_{(001)}$ of 1.4 nm, which represents the thickness of one saponite layer, plus an interlayer space filled with sodium cations surrounded by two water layers. In the DOPA–saponite composite, (001) and (002) reflections are observed at 8 and 4° (2θ) corresponding to reticular distances of 1.1 and 2.2 nm, respectively. It is most likely that the 1.1 nm value corresponds to the second-order diffraction peak of the 2.2 nm one. Therefore, the samples contain stackings of saponite layers with interlayer spacings much superior to the pristine clays, indicative of intercalation.

On the basis of the basal spacing $d_{(001)}$ of 2.2 nm and subtracting the thickness of the saponite layer (0.96 nm), the interlayer space is calculated to be 1.28 nm. This spacing can be accounted for if the L-DOPA molecules are accommodated vertically in the interlayer region as a bilayer of partially interdigitated species.

DOPA is a tetra-acid with the following pK_a values: 2.32 (−COOH), 8.72 ($-NH_3^+$), 9.96 (phenolic −OH), and 11.79 (second phenolic −OH). In the deposition solution, speciation favors the zwitterion $H_3DOPA^{\pm}$ (bearing one ammonium and one carboxylate group), with a minor amount of the monoanion H_2DOPA^-. Zwitterions probably have only a weak electrostatic interaction with the clay material, which bear a substitutional negative charge, and at any rate they cannot compensate the negative charge of the layers. The question of the driving force for their intercalation remains therefore open.

In our previous experimental work where intercalation was observed, it was speculated that hydrophobic interactions between parallel aromatic rings of DOPA molecules in the interlayer contributed to stabilize the intercalated forms. There were also indications, however, of hydrogen bonding between catechol functions OH groups of the saponite layers edges.[26] The latter type of interaction is more difficult to investigate because it is not visible by XRD, and in addition the edge OH content is variable.

The TG and DTG curves in Figure 3 may be separated in three regions. In the 50–100 °C range, a large weight loss associated with an endothermic process corresponds to the elimination of physisorbed water (including interlayer water for

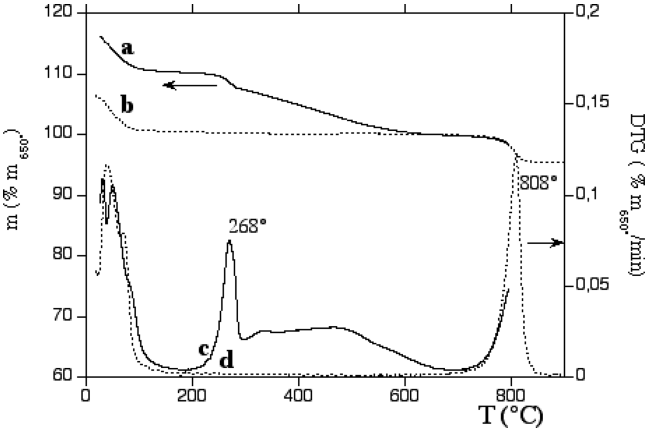

Figure 3. TG (left scale, in weight % of residual mass at 650 °C) of (a) DOPA/saponite and (b) raw Na^+-saponite; DTG (right scale) of (c) DOPA/saponite and (d) raw Na^+-saponite.

dx.doi.org/10.1021/jp3094148 | J. Phys. Chem. C XXXX, XXX, XXX–XXX

Table 1. Calculated and Experimental Super Cell Parameters and Energy of Saponite[a]

structural formula Na-saponite	a	b	c	α	β	γ
$Na_1[Mg_6(Si_7Al_1)O_{20}(OH)_4]$	0.536	0.927	1.021	87.4	101.2	90.0
Exp.[53]	0.530	0.914	0.970−1.021	90.1	97.00	90.0

[a]Distances in nanometers, angles in degrees.

the saponite). The amount of water lost in this step corresponds to 5.8% (approximately five water molecules). Between 150 and 650°, thermal events are only apparent for the DOPA-containing composites and may thus be attributed to the elimination of DOPA-derived organic matter: two successive maxima are observed, respectively, in the 250−280 and 400−500° ranges. Quantification of these events indicates that organic matter amounts to 9.8 wt %, as related to the inorganic matrix for DOPA−saponite. This may be compared with the amount of DOPA introduced in the dispersion, that is, 24 wt % with respect to the mass of the matrix. As already previously reported, the initially translucent dispersion of DOPA−saponite turned pink 30 min after contact and black after 24 h. The observed color changes are easy to understand: the initial red coloration is due to the oxidation of the catechol function to quinone, and the darkening is due to the appearance of polyaromatics upon polymerization. It is assumed that most of the polyaromatics form in the liquid phase because after filtration a black filtrate containing the polymerized molecule is recovered.

Finally, at 826 °C, a sharp event is observed that has been attributed to a dehydroxylation event, leading to a phase transition to enstatite. (This was verified by XRD of the calcined material.[25])

TEM micrographs exhibit stacked layers with two different $d_{(001)}$ values: 1.1 and 2.2 nm.

Molecular Modeling Results. *a. Clay Structure.* The best agreement with the experiment for the geometrical parameters was obtained with exchange-correlation energies treated using the generalized gradient approximations (GGAs) by Perdew and Wang (PW91). The geometry differences determined with LDA and GGA approaches were small. Finally, the GGA approach was retained, as it is generally found to give more reliable adsorption energies for a range of molecules on phyllosilicates[49,50] as well as for the physical properties of water[51] and other hydrogen bonded systems.[52] Monkhorst−Pack k-point convergence was performed, resulting in an optimal mesh of 6 × 2 × 1. As shown in Table 1, unit cell equilibrium lattice parameters showed good agreement with experimental results,[53] within 1%.

b. Hydration. Most studies of clay minerals swelling have been carried out with fixed a and b cell parameters, where only the c vector or basal spacing ($d_{(001)}$) (perpendicular distance between layers = z component of the c vector) varied. In the present study, all geometrical parameters were relaxed in the energy optimization procedure.

To study the presence of water molecules in the clay interlayer space, we undertook a systematic procedure of adding pairs of water molecules in the (1 × 2 × 1) supercell. The same unit cell was used later to study L-DOPA adsorption. After having carefully chosen the starting geometries for optimization, the water adsorption energies were calculated. In Figure 2, the mean adsorption energy per water molecule is plotted versus the number of water molecules per unit cell (1 × 1 × 1).

The adsorption of a single water molecule per unit cell is very favorable due to direct cation−dipole interaction between the Na^+ cation and water molecule; in chemical terms, this can be viewed as coordinative binding. Beyond that point, the following steps of water addition were still much favored; that is, they were more favorable than water liquefaction (see below), and they were accompanied by an increase in the number of water molecules coordinated to Na^+. A maximum in the absolute adsorption energy was found at four water molecules per unit cell: the energy of adsorption between three and four water molecules per unit cell was −0.63 eV/water molecule (−60.8 kJ mol^{-1}; see Figure 2). This hydration rate is very close to the experimentally found one: four to five water molecules/unit cell. It is interesting to note that the adsorption energy of water evolves asymptotically toward the autosolvation energy of water. In our model, one can notice the beginning of a convergence toward −0.55 eV (−53.0 kJ mol^{-1}; see Table 2),

Table 2. Adsorption Energy of Water and L-DOPA in Saponite for Different Degrees of Hydration Calculated Using Equations 4 and 5[a]

no. water molecules/unit cell	$\Delta E_{ads}(H_2O)$	ΔE_{ads}(L-DOPA)
0[b]		−0.48
1[b]	−0.69	−0.41
2[b]	−0.58	−0.38
3	−0.62	−0.53
4	−0.63	−0.40
5	−0.63	−0.25
6	−0.61	−0.31
7	−0.57	−0.86
8	−0.56	−0.98
9	−0.53	−1.36
10	−0.53	−1.75

[a]Energies in electronvolts. [b]DOPA in neutral configuration, other in zwitterionic form.

which is in agreement with results using the autosolvation energy of water calculated with continuum solvation models[54] (for the sake of comparison, the experimental autosolvation energy of water is −0.28 eV or −27.0 kJ mol^{-1}).[55] Of course, one should not forget that water molecules do not belong to a bulk phase but are sandwiched between clay layers and therefore constitute a confined water phase. The high stabilizations calculated for the first water molecules in our model mean that the saponite is a hydrophilic material, and this is largely due to the presence of the cations in the interlayers. The cations are positioned next to two oxygen atoms of basal hexagonal Si/Al rings. Because of the chosen Si/Al ratio of 7, one Na^+ is situated close to a six ring containing two Al atoms. Both Na^+ cations have a coordination of about 5 (two basal oxygen atoms and three water molecules) in the system containing four molecules of water per unit cell. The system containing five water molecules is found to be slightly less stable (by 0.05 eV/water molecule or 4.8 kJ.mol^{-1}) than the system containing four molecules of water; this energy

dx.doi.org/10.1021/jp3094148 | J. Phys. Chem. C XXXX, XXX, XXX−XXX

difference is within the accuracy of the calculation. In this system, the Na^+ cation is reaching a coordination number of six.

The relation of the interlayer distance to water insertion is shown in Figure 4. The *c* parameter increases almost linearly

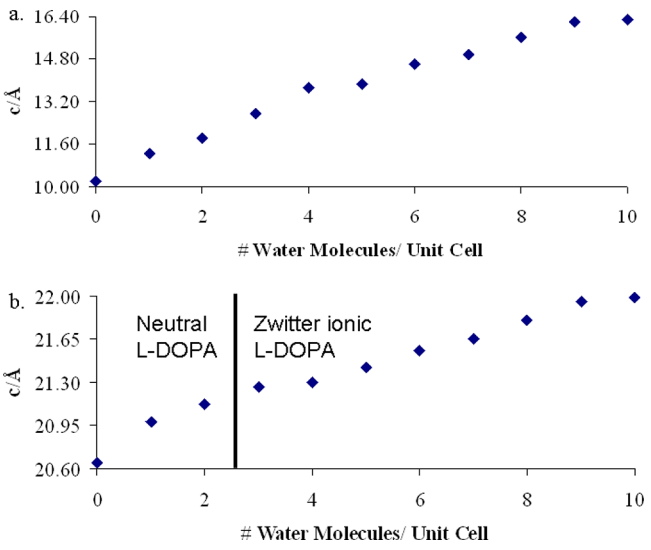

Figure 4. Calculated cell parameter *c* of saponite without (a) and with (b) L-DOPA versus water content.

from 0 to 10 water molecules, going from 1.021 to 1.629 nm. These calculated *c* parameters may be compared with experimental results. The dry saponite has an experimental *c* parameter of 0.980 nm,[56] close to the calculated value of 1.021 nm without water molecules. Another stable form is observed for intermediate hydration at 1.2 nm. It is called the "one water layer" form and thought to correspond to three-coordinated Na^+ ions. It would correspond to the calculated value for two to three water molecules per unit cell and thus per Na^+ ion.

In the experiments reported here a *c* parameter of 1.4 nm is measured from the d_{001} value.[26] The experimental value would correspond, according to our theoretical graph, with the presence of four or five water molecules per unit cell (respectively, corresponding to 1.371 and 1.385 nm). Our TGA experiments show[26] the presence of approximately five water molecules per unit cell: the calculated *c* parameter is in very good agreement with the experimental one. In conclusion, one can say that the model presented in this work predicts well-stable configurations of hydrated saponite at the molecular level.

c. L-DOPA Adsorption. To study the adsorption of L-DOPA, two molecules were inserted between the interlayer of the clay material represented by a (1 × 2 × 1) saponite unit cell, together with an increasing number of water molecules (0 to 10 per unit cell). Two unit cells were used as a super cell to improve the symmetry and increase the degrees of freedom of the system.

Two modes of adsorption were first considered: (a) standing up and (b) lying down in the interlayer. Although the experimental interlayer distance suggests that the L-DOPA molecules adsorb perpendicularly to the clay layer surfaces (standing up), it was interesting to see if a confirmation was found from the theoretically derived energetics. Indeed, after optimization, the respective adsorption/interaction energies of L-DOPA with the clay interlayer are 0.30 eV (28.9 kJ mol^{-1}) in favor of the "standing up" adsorption geometry under dry conditions, (for the neutral form of L-DOPA, not the zwitterionic one, see below). For the hydrated case (zwitterionic form of L-DOPA), the same result was found. Nevertheless, it should be noted that the energy differences found between both geometries are relatively small and are on the limit of the accuracy of the calculation level used in this calculation. From the investigation and visualization of the nonlocal interactions such as dispersion interactions,[57,58] which can be estimated from the PBE electron density, it can be shown that the interactions between the L-DOPA molecules stabilize the standing up geometry by what is often called $\pi-\pi$ stacking.[59]

The energetically most favorable geometry (Table 2 and Figure 5) found for the standing-up molecules containing three

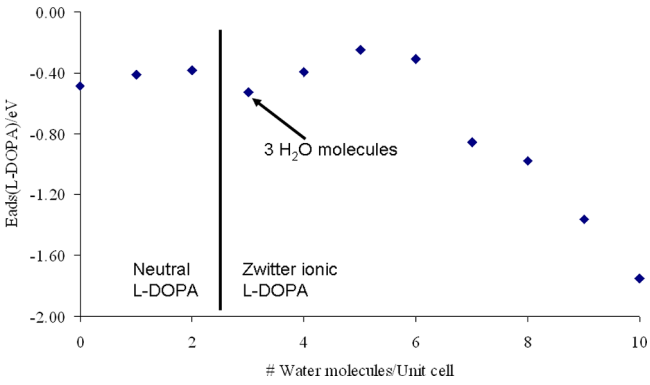

Figure 5. Calculated adsorption energy of one L-DOPA molecule per water molecule added within the clay layers in a single unit cell.

water molecules per L-DOPA molecule has the following features (Figure 6): L-DOPA is found to adsorb via its catechol moiety, which is close to the basal clay surface. It is actually bound in a cooperative way, involving several interactions. First, there is a direct H-bonding between one of the phenolic groups and an oxide of the layer surface; this phenolic group also directly coordinates to a neighboring Na^+ cation. The second phenolic group is indirectly bound to the clay layer, via a hydrogen-bonded water molecule. Finally the carboxylic group is interacting with one water molecule, which is on its turn interaction with another water molecule in interaction with the sodium cation and the layer surface.

It is clear that the water molecules are all located close to the clay basal surface and not between the L-DOPA aromatic rings.

We have studied other conformations of perpendicular DOPA molecules, where the carboxylic acid/carboxylate moiety was closer to the clay layer than the catechol end (simultaneous interaction through both groups is not compatible with the interlayer spacing). The interaction energy difference between an adsorption via the catechol moiety or the carboxylate group is about 0.15 ± 0.10 eV, over the range of 0−10 water molecules per unit cell, in favor of the catechol moiety, in agreement with experiment.[25]

Interesting results on the solvation of L-DOPA molecules in the interlayer of Na-saponite are found when the degree of hydration is varied. Under "dry" conditions (no added water, L-DOPA is more stable in its neutral form, H_3DOPA with −COOH and $-NH_2$ functions (adsorption energy −0.48 eV or −46.3 kJ mol^{-1}), than in its zwitterionic form ($H_3DOPA^{\pm}$ with $-COO^-$ and $-NH_3^+$, adsorption energy −0.20 eV or −19.3 kJ mol^{-1}). Progressively increasing the number of water molecules

dx.doi.org/10.1021/jp3094148 | J. Phys. Chem. C XXXX, XXX, XXX−XXX

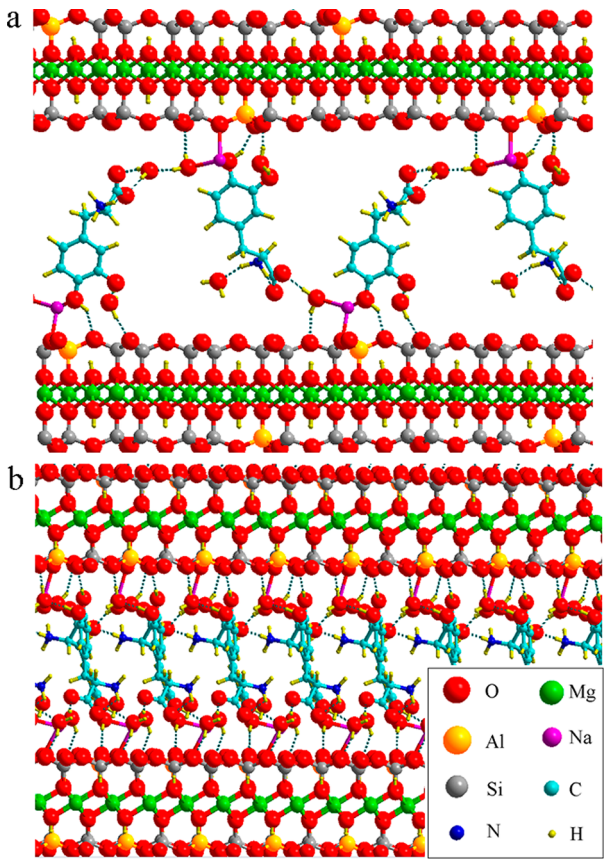

Figure 6. Most stable hydrated L-DOPA/saponite composite model ((a) *xz* plane, (b) *yz* plane).

leads to a relative stabilization of the zwitterion. This switch is observed after adding three water molecules per unit cell.

Such a behavior was not unexpected. Indeed, it has long been known that a minimum number of water molecules is required to stabilize the zwitterionic form of amino acids over the neutral one, and the question has been studied in detail in the case of glycine.[60−63] Furthermore, Rimola et al. have shown that even when glycine is adsorbed on silica a minimum number of microsolvating water molecules is still necessary to stabilize the zwitterion.[64] Obviously, this rule is also valid for L-DOPA in a smectite clay.

The hydration corresponding to the neutral-zwitterionic transition corresponds to a local minimum in the adsorption energy (most negative value) for L-DOPA (see Figure 5), but after adding six molecules of water per unit cell, the L-DOPA interaction energy increases further (the adsorption energy becomes more negative). An H-bond network involving not only the water molecules but also the amino, carboxylic, and catechol groups of L-DOPA stabilizes the system.

The supercell geometry depends on the water content as follows (See Table 2 and Figure 4): In its dehydrated form, the unit cell parameter *c* is found to be 2.064 nm. When a first water molecule is introduced between the saponite layers containing L-DOPA, the *c* parameter increases by 0.035 nm. Further hydration of the system increases the unit cell parameter *c* by 0.015 nm for each water molecule added to the system. One may recall that for the hydrated system without L-DOPA the *c* parameter increases almost linearly with the increase in the number of water molecules per unit cell.

Experimentally a *c* value of ∼2.2 nm is observed, which would correspond experimentally with a water content of three molecules per unit cell. According to the experiment,[26,3] the water uptake in saponite corresponds usually to two water molecules per unit cell up to a maximum of six molecules, corresponding to 4−12 in the (1 × 2 × 1) super cell. In our previous paper,[25] we obtained experimentally three water molecules per unit cell, which is in good agreement with our present theoretical results (three water molecules coadsorbed with L-DOPA, see Figure 6). The theoretically calculated *c* parameter corresponding to the uptake of three water molecule is equal to 2.127 nm. As in the case of the pure water/clay system (cf. supra), the calculated *c* parameter value is close to the experimentally observed one based on the experimental error, on one hand, and the computational error due to the complexity of the calculation, on the other hand (a few hundredths of a nanometer difference).

The particular self-assembly of L-DOPA molecules in Na-saponite that has been characterized on the molecular level in this study can serve as a basis for understanding and improving the vectorization applications. Indeed, the L-DOPA concentration in the clay material can be altered by changing the exchangeable cation type or the type of clay. Controlling the hydration rate and the adsorption energy of L-DOPA will enable us to fine-tune the delivery rate of the bioorganic molecule in pharmaceutical applications.

5. CONCLUSIONS

Experimental and theoretical results are confronted to elucidate the molecular structure of the intercalation of L-DOPA in the interlayer space of saponite. The adsorption geometry of L-DOPA (standing up or lying down in the interlayer) was studied, and the effect on the neutral/zwitterionic form of L-DOPA on the interaction with the clay and the degree of hydration with and without the presence of L-DOPA in the interlayer space were carefully analyzed by means of periodic DFT.

The hydration states of the pure Na-saponite and the composite were specifically studied, and the optimum water content was determined. Experimental and theoretical results were found to be in very good agreement with the thermal analysis experiment. For the pure Na-clay system, four to five water molecules per unit cell were found to be an optimum degree of hydration, whereas in the composite L-DOPA/clay up to three water molecules were found to agree with the adsorption energies and unit cell parameters. The adsorption energy of the molecule of L-DOPA has been found to be equal to 0.48 eV per molecule, which is an important parameter for vectorization applications.

The next step in this investigation will be the analysis of the reactivity of L-DOPA in the particular environment of hydrated Na-saponite because the formation of polymer molecules by reaction with dissolved O_2 has been observed experimentally. Dynamic modeling might also shed some light in the transport properties and diffusion of water, cations, and dioxygen in the clay system. Finally, if oxidative polymerization can be avoided, then it will be interesting to determine if a trigger of such a pH change may modify the adsorption energy and therefore if controlled release can be achieved.

AUTHOR INFORMATION

Corresponding Author

*E-mail: frederik.tielens@upmc.fr, vtimon@iact.ugr-csic.es.

dx.doi.org/10.1021/jp3094148 | *J. Phys. Chem. C* XXXX, XXX, XXX−XXX

Notes

The authors declare no competing financial interest.

■ ACKNOWLEDGMENTS

This work was performed using HPC resources from GENCI-[CCRT/CINES/IDRIS] (Grant 2012-[x2012082022]) and the CCRE of Université Pierre et Marie Curie. It was carried out under the HPC-EUROPA2 project (project number: 477) with the support of the European Commission Capacities Area - Research Infrastructures Initiative. Dr. B. Diawara from LCPS ENS Paris is kindly acknowledged for providing us with *ModelView* used in the visualization of the structures.

■ REFERENCES

(1) Lauzon, R. V. *Oil Gas J.* **1984**, *82*, 175−179.
(2) Poncelet, G.; Fripiat, J. J. Chapter 1. In *Handbook of Heterogeneous Catalysis*, 2nd ed.; Wiley-VCH: Weinheim, Germany, 2008; pp 219−247.
(3) Sanchez, C.; Julian, B.; Belleville, P.; Popall, M. *J. Mater. Chem.* **2005**, *15*, 3559−3592.
(4) Statz, A. R.; Meagher, R. J.; Barron, A. E.; Messersmith, P. B. *J. Am. Chem. Soc.* **2005**, *127*, 7972−7973.
(5) Lee, H.; Lee, B. P.; Messersmith, P. B. *Nature* **2007**, *448*, 338−341.
(6) Hedges, J. I.; Hare, P. E. *Geochim. Cosmochim. Acta* **1987**, *51*, 255−259.
(7) Di Leo, P. *Clays Clay Min.* **2000**, *5*, 495−502.
(8) Kalra, S.; Pant, C. K.; Pathak, H. D.; Mehta, M. S. *Ind. J. Biochem. Biophys.* **2000**, *37*, 341−346.
(9) Mallakpour, S.; Dinari, M. *Appl. Clay Sci.* **2011**, *51*, 353−359.
(10) Cuadros, J.; Aldega, L.; Vetterlein, J.; Drickamer, K.; Dubbin, W. *J. Colloid Interface Sci.* **2009**, *333*, 78−84.
(11) Fraser, D. G.; Jakschitz, D. F. T.; Rode, B. M. *Phys. Chem. Chem. Phys.* **2011**, *13*, 831−838.
(12) Mignon, P.; Ugliengo, P.; Sodupe, M. *J. Phys. Chem. C* **2009**, *113*, 13741−13749.
(13) Mignon, P.; Sodupe, M. *Phys. Chem. Chem. Phys.* **2012**, *14*, 945−954.
(14) Michalkova, A.; Robinson, T. L.; Leszczynski, J. *Phys. Chem. Chem. Phys.* **2011**, *13*, 7862−7881.
(15) Chatterjee, A.; Ebina, T.; Mizukami, F. *J. Phys. Chem. B* **2005**, *109*, 7306−7313.
(16) Ferris, J. P.; Hill-Jr, A. R.; Liu, R.; Orgel, L. E. *Nature* **1996**, *381*, 59−61.
(17) Lambert, J.-F. *Origins Life Evol. Biospheres* **2008**, *38*, 211−242.
(18) Nutt, J. G.; Obeso, J. A.; Stocchi, F. *Trends Neurosci.* **2000**, *23*, S109−115.
(19) Cools, R. *Neurosci. Biobehav. Rev.* **2006**, *30*, 1−23.
(20) Antonini, A.; Bondiolotti, G.; Natuzzi, F.; Bareggi, S. R. *Eur. Neuropsychopharmacol.* **2010**, *20*, 683−687.
(21) Muzzi, C.; Bertocci, E.; Terzuoli, L.; Porcelli, B.; Ciari, I.; Pagani, R.; Guerranti, R. *Biomed. Pharmacother.* **2008**, *62*, 253−258.
(22) Paris, I.; Martinez-Alvarado, P.; Cardenas, S.; Perez-Pastene, C.; Graumann, R.; Fuentes, P.; Olea-Azar, C.; Caviedes, P.; Segura-Aguilar, J. *Chem. Res. Toxicol.* **2005**, *18*, 415−419.
(23) Park, T.-J.; Kim, J.; Kim, T.-K.; Park, H.-M.; Choi, S.-S.; Kim, Y. *Bull. Korean Chem. Soc.* **2008**, *29*, 2459−2464.
(24) Wei, M.; Pu, M.; Guo, J.; Han, J.; Li, F.; He, J.; Evans, D. G.; Duan, X. *Chem. Mater.* **2008**, *20*, 5169−5180.
(25) Jaber, M.; Bouchoucha, M.; Delmotte, L.; Méthivier, C.; Lambert, J.-F. *J. Phys. Chem. C* **2011**, *115*, 19216−19225.
(26) Jaber, M.; Lambert, J.-F. *J. Phys. Chem. Lett.* **2010**, *1*, 85−88.
(27) Kim, S.; Beum, S. *Langmuir* **2010**, *26*, 14730−14736.
(28) Furubayashi, A.; Hiradate, S.; Fujii, Y. *J. Chem. Ecol.* **2007**, *33*, 239−250.
(29) Folliet, N.; Roiland, C.; Begu, S.; Aubert, A.; Mineva, T.; Goursot, A.; Selvraj, K.; Duma, L.; Tielens, F.; Mauri, F.; Laurent, G.; Bonhomme, C.; Gervais, C.; Babonneau, F.; Azaïs, T. *J. Am. Chem. Soc.* **2011**, *133*, 16815−16827.
(30) Lopes, I.; Piao, L. Y.; Stievano, L.; Lambert, J.-F. *J. Phys. Chem. C* **2009**, *113*, 18163−18172.
(31) Fraser, D. G.; Greenwell, H. C.; Skipper, N. T.; Smalley, M. V.; Wilkinson, M. A.; Deme, B.; Heenan, R. K. *Phys. Chem. Chem. Phys.* **2011**, *13*, 831−838.
(32) Bujdak, J.; Remko, M.; Rode, B. M. *J. Colloid Interface Sci.* **2006**, *294*, 304−308.
(33) Hazen, R. M. *Am. Mineral.* **2006**, *91*, 1715−1729.
(34) Jaber, M.; Miehe-Brendle, J.; Delmotte, L.; Le Dred, R. *Solid State Sci.* **2005**, *7*, 610−615.
(35) Benetoli, L. O. B.; de Souza, C. M. D.; da Silva, K. L.; de Souza, I. G. J.; de Santana, H.; Paesano, A. J.; da Costa, A. C. S.; Zaia, C. T. B. V.; Zaia, D. A. M. *Origins Life Evol. Biospheres* **2007**, *37*, 479−493.
(36) Siffert, B.; Naidja, A. *Clay Minerals* **1992**, *29*, 109−118.
(37) Kresse, G.; Hafner, J. *Phys. Rev. B* **1993**, 558−561.
(38) Kresse, G.; Hafner, J. *Phys. Rev. B* **1994**, *49*, 14251−14269.
(39) Perdew, J. P.; Chevary, J. A.; Vosko, S. H.; Jackson, K. A.; Pederson, M. R.; Singh, D. J.; Fiolhais, C. *Phys. Rev. B* **1992**, *46*, 6671−6687.
(40) Perdew, J. P.; Burke, K.; Ernzerhof, M. *Phys. Rev. Lett.* **1996**, *77*, 3865−3868.
(41) Perdew, J. P.; Burke, K.; Ernzerhof, M. *Phys. Rev. Lett.* **1997**, *78*, 1396−1396.
(42) Tielens, F.; Gervais, C.; Lambert, J.-F.; Mauri, F.; Costa, D. *Chem. Mater.* **2008**, *20*, 3336−3344.
(43) Calatayud, M.; Tielens, F.; De Proft, F. *Chem. Phys. Lett.* **2008**, *456*, 59−63.
(44) de Bocarmé, T. V.; Chau, T.-D.; Tielens, F.; Andrés, J.; Gaspard, P.; Wang, L. R. C.; Kreuzer, H. J.; Kruse, N. *J. Chem. Phys.* **2006**, *125*, 054703.
(45) Tielens, F.; Andrés, J. *J. Phys. Chem. C* **2007**, *111*, 10342−10346.
(46) Tielens, F.; Trejda, M.; Ziolek, M.; Dzwigaj, S. *Catal. Today* **2008**, *139*, 221−226.
(47) Blöchl, P. E.; Jepsen, O.; Andersen, O. K. *Phys. Rev. B* **1994**, *49*, 16223−16233.
(48) Kresse, G.; Joubert, J. *Phys. Rev. B* **1999**, *59*, 1758−1775.
(49) Sainz-Díaz, C. I.; Francisco-Márquez, M.; Vivier-Bunge, A. *Theor. Chem. Acc.* **2010**, *125*, 83−95.
(50) Clausen, P.; Andreoni, W.; Curioni, A.; Hughes, E.; Plummer, C. J. G. *J. Phys. Chem. C* **2009**, *113*, 12293−12300.
(51) Grossman, J. C.; Schwegler, E.; Draeger, E. W.; Gygi, F.; Galli, G. *J. Chem. Phys.* **2004**, *120*, 300−311.
(52) Ireta, J.; Neugebauer, J.; Scheffler, M. *J. Phys. Chem. A* **2004**, *108*, 5692−5698.
(53) Pizzarello, S.; Cronin, J. R. *Geochim. Cosmochim. Acta* **2000**, *64*, 329−238.
(54) Bryantsev, V. S.; Diallo, M. S.; Goddard, W. A. I. *J. Phys. Chem. B* **2008**, *112*, 9709−9719.
(55) NIST Standard Reference Database Number 69. In *NIST Chemistry WebBook*; National Institute of Standards and Technology: Washington, DC, June 2005.
(56) Suquet, H.; Pezerat, H. *Clays Clay Miner.* **1987**, *35*, 353−362.
(57) Johnson, E. R.; Keinan, S.; Mori-Sánchez, P.; Contreras-García, J.; Cohen, A. J.; Yang, W. *J. Am. Chem. Soc.* **2010**, *132*, 6498−6505.
(58) Contreras-García, J.; Johnson, E.; Keinan, S.; Chaudret, R.; Piquemal, J.-P.; Beratan, D.; Yang, W. *J. Chem. Theory Comput.* **2011**, *7*, 625−632.
(59) Contreras-García, J. Personal communication, 2012
(60) Jensen, J. H.; Gordon, M. S. *J. Am. Chem. Soc.* **1995**, *117*, 8159−8170.
(61) Tortonda, F. R.; Pascual-Ahuir, J. L.; Silla, E.; Tunón, I. *Chem. Phys. Lett.* **1996**, *260*, 21−26.
(62) Ramaekers, R.; Pajak, J.; Lambie, B.; Maes, G. *J. Chem. Phys.* **2004**, *120*, 4182−4193.
(63) Aikens, C. M.; Gordon, M. S. *J. Am. Chem. Soc.* **2006**, *128*, 12835−12850.

632 (64) Rimola, A.; Civalleri, B.; Ugliengo, P. *Langmuir* **2008**, *24*,
633 14027−14034.